FLAME AEROSOL SYNTHESIS OF NANOALUMINA

[1*]Frank, L. M. and [2]Shaka, S. O.
[1]*General Studies Department, International Institute of Tourism and Hospitality*
Yenagoa, Bayelsa State, Nigeria
[2]*Department of Physics, Federal University of Petroleum, Effurun, Delta State, Nigeria*
*Corresponding author email: lalas452000@yahoo.co.uk

ABSTRACT

The synthesis of all types of industrial products depends of the specific combination of applied methods and the conditions of syntheses (i.e. temperature of flame, flow rates, quality of precursors, the chemical compositions of gaseous and liquid precursors, etc.); the product will then show high quality and high performance level for further treatment. The availability of equipment also determines the methods of synthesis and therefore equipment which is able to provide suitable condition for production of materials is best. In this research, an assembly of equipment is constructed to obtain a perfect production. By adjusting the temperature condition of the flame using the Flame Spray Pyrolysis (FSP) method of synthesis, and keeping every other conditions of synthesis constant, high quality performance agglomerate-free nano-sized Al_2O_3 particles with a size range of 5-30nm were synthesized and compared. The precursors and the resultant oxide powders were characterized by chemical analysis, X-ray diffraction (XRD). The result of this further experiment shows evidence of stable nano-alumina, which further confirms that flame spray pyrolysis method can successfully be used to synthesize nano-size Al_2O_3. However, high quality performance of the synthesized nano-sizeAl_2O_3 particle with 750^{o}C is greater than those synthesized with either 450^{o}C or 600^{o}C temperature of flame.

Keywords: Pyrolysis, Nano-size, Agglomerate-free, Nano-alumina.

INTRODUCTION

Nanostructured particles are a wide range of materials that is probably still widely unexplored and thus provides a fascinating area of study for many researchers. It is a research area that is wide and has many potential applications (Wu *et al*, 2001). These particles are numerous, both at basic level and high level, these particles have been explored and are still under investigation by many researchers, leaving large space for thorough scientific analysis, which of course requires long term ultimate conclusions, in the mean, nanostructured particles will remain the fascination of many scientist world over, being able to fabricate these particles presents its peculiar challenges thus require further research.The potential application fields of nanoparticles are very wide and, probably, not yet fully understood: from energetics (sensors, propulsion, and reduction of environmental impact) to chemistry (catalysis, additives) to medicine (diagnostics) and of course to material science. Also the problem of nanoparticles impact on human health is a rather unexplored field. Thus caution is applied in their exploration and uses. The same can be said about the study of the different methodologies for controlled synthesis of nanoparticles. In fact, numerous processes are utilized for the synthesis of nanostructured materials and in particular for nanoparticle production.

This research work aims at the synthesis of agglomerate free nanostructured particles, in this case nano alumina. Aerosol processes are used routinely for the commercial production of ultrafine particles (dp< 100 nm) and materials fabricated from them, and for pilot and laboratory scale production as well. Aerosol reaction engineering refers to the design of such processes, with the goal of relating product properties to the material properties of the aerosol precursors and the process conditions. The most important process conditions are usually the aerosol volume concentration (volume of particles per unit volume of gas) and the time/ temperature history of the system.

Fine particle formation by aerosol processes almost always takes place by gas-to-particle conversion. Condensable molecules produced by physical or chemical processes self-nucleate to form particles. The nuclei may be as small as a single molecule for refractory materials, but subsequent collision and coalescence leads to the formation of larger particles. Many lab-scale studies have been made to demonstrate novel methods for particle synthesis or to elucidate the mechanisms of particle formation.

METHODOLOGY

Flame spray pyrolysis is a one-step process in which a liquid feed – a metal precursor(s) dissolved in a solvent is sprayed with an oxidizing gas into a flame zone. The spray is combusted and the precursor(s) are converted into nanosized metal or metal oxide particles, depending on the metal and the operating conditions. The technique is flexible and allows the use of a wide range of precursors, solvents and process conditions, thus providing control over particle size and composition. Summarily, flame spray pyrolysis is the aerosol process that atomizes a solution and heats the droplets to produce solid particles (Overney, 2010).

Flame spray pyrolysis can be used to produce a wide array of high purity nanopowders ranging from single metal oxides such as alumina to more complex mixed oxides, metals and catalysts. The technique was first developed by the research group of Sotiris E. Pratsinis at ETH Zurich, Switzerland (Strobel*et al*., 2006). Since then it has been used to create new and sophisticated materials for catalysis and other applications (Strobel*et al*., 2009). Nano particles can be produced, depending on the material composition, and a number of process variables enable the preparation of well-defined target materials.

In this study we investigate a burner with a premixed flame of different temperatures, in which fuel, acetylene and oxygen with liquid-fed volatilized precursors are intermixed at the molecular level when ignition occurs. The particles are then blown with a fan through a metal tube and collected in a high voltage electrostatic precipitator in the collection chamber.

There are several methods used for synthesizing nanostructured particles but the Flame Spray Pyrolysis (FSP) method which involves premixed flame (acetylene and oxygen) at a controlled level was used in this research. The experimental setup was constructed and fabrication of powder was achieved at the end of the experiment.

Further analysis or characterization of the samples fabricated from the experimental setup using X-ray Diffraction (XRD) shows stability of nanostructured substance synthesized, verifying that nanostructured particles can be synthesized using Flame Spray Pyrolysis method.

This work deals with the experimental preliminary work done in the production of nano particles using flame spray pyrolysis method of synthesizing nano alumina. The method involves the use of commercial anhydrous Aluminum trichloride ($AlCl_3$) powder (purity 99.7%) from Mark, Germany as starting material. Figure.1 presents a schematic illustration of the flame spray pyrolysis (FSP) apparatus used to prepare the Al_2O_3 nano-particles. The apparatus consist of an in-house manufactured heating chamber, a flame gun, in-house manufactured powder combustion and collection chamber which consists of an electrostatic precipitator, powered by a high voltage power source; a fan and an ultrasonic atomizer both powered by the high voltage power source. The liquid saturated $AlCl_3$ powder was fed into the flame using an ultrasonic atomizer powered by the high voltage source. The heating chamber was kept as 300 ^{O}C and temperature was increased gradually and collection was done in the collection chamber. The purity of the sample collected was also analyzed.

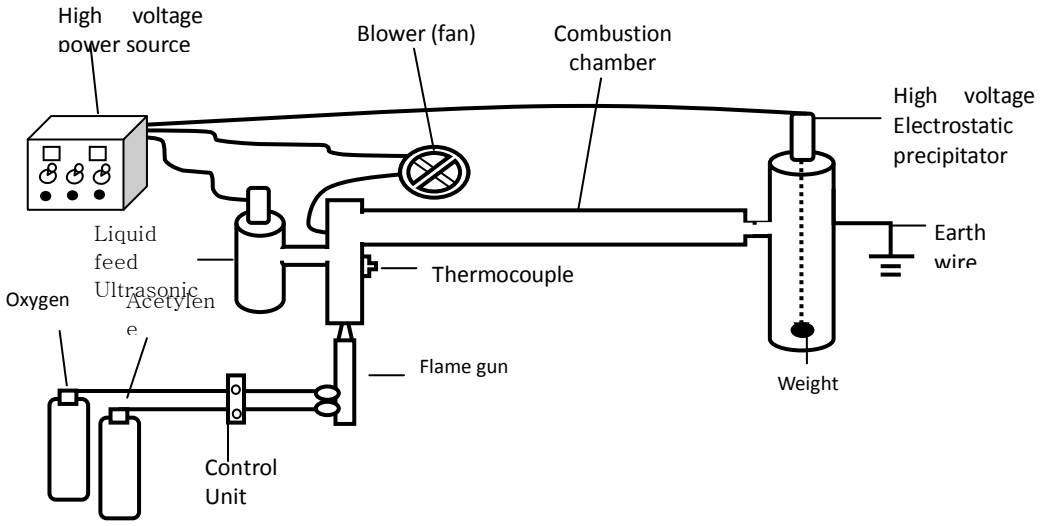

Figure 1: Schematic diagram of Flame Spray Pyrolysis (FSP) equipment

Figure 1 shows the experimental setup of in-house equipment used as flame spray pyrolysis (FSP) equipment. The equipment consist of liquid-feed 30 watts ultrasonic atomizer with capacity of 30 ml with frequency of 1.66 Hz, containing the precursor saturated $AlCl_3$, having a flow rate of 1 ml/min. Also in the diagram are the controlled propane and oxygen gases. Power source of 2000 V, supplies power to the ultrasonic atomizer, the fan (blower) and the high voltage electrostatic precipitator, the electronic controller hinged to a thermocouple connected to aluminum tube (combustion chamber) is to ensure that temperature drop does not lead to changes in the combustion chamber. A second electronic controller hinged to thermocouple is connected to the flame chamber records the temperature of flame using the melting point of various metals. The flow rate of the acetylene and oxygen premixed gas is kept at 20 mmHg, 30 mmHg, 40 mmHg for all three samples respectively.

The liquid precursor in the ultrasonic atomizer is atomized and the molecules directly into the ignited flame, combustion takes place and the gas particles are blown by the centrifugal fan through the stainless steel capillary tube of diameter 50 mm (outer diameter) and 40 mm (inner diameter).

The apparatus is designed in order to achieve, through the longitudinal displacement of the dispersion gas injector, a vartion of the outflow area, from zero to the maximum value. By maintaining constant the exit area, the dispersion gas flow rate depends on the upstream applied pressure till the critical value is achieved. The pressure in the dispersing gas supply chamber was monitored in order to operate always below such critical level.

The combustion gases are conveyed through the pipe and collected by the electrostatic precipitator. The electrostatic precipitator is earthed. The aluminum cylinder is then vibrated to collect the nanoparticles for further treatment. As a rule the temperature in the aluminum pipes are kept at 300°C. Excess heat leads to starvation mode, where there will be less precursor left in the furnace.

Precursor Liquid Composition

The precursor composition is a key parameter in flame spray pyrolysis (FSP) in order to achieve the preferred product properties. The choice of precursor depends on cost, reactivity, selectivity, stability before processing, and low toxicity. Saturated $AlCl_3$ was chosen as precursor because of its availability, and low toxicity (chlorine gas was given off as gaseous residue), the precursor was fed into a liquid fed ultrasonic atomizer, the equipment consist of liquid-feed 30 watts ultrasonic atomizer with capacity of 30ml with frequency of 1.66 Hz containing the precursor saturated $AlCl_3$, having a flow rate of 1 ml/min.

Ultrasonic Atomizer

Ultrasonic spray pyrolysis is employed to generate an aerosol from a dilute aqueous metal salt solution ($AlCl_2$), resulting in the production of particles with a narrow size distribution. A review by Messing *et al*. (1993) shows the use of spray pyrolysis in the synthesis of particles of micron size, producing various metal powders. Therefore, ultrasonic atomizer was used to produce molecules sprayed directly into flame.

The effect of precursor concentration on the particle size was weak and mostly dependent on the aerosol droplet size; ultrasonic spray pyrolysis has been most used to synthesize fine powders by aerosol decomposition.

Process Flow Diagram

The process flow diagram shows the processes involved in the synthesis of nano alumina using Flame Spray Pyrolysis (FSP).

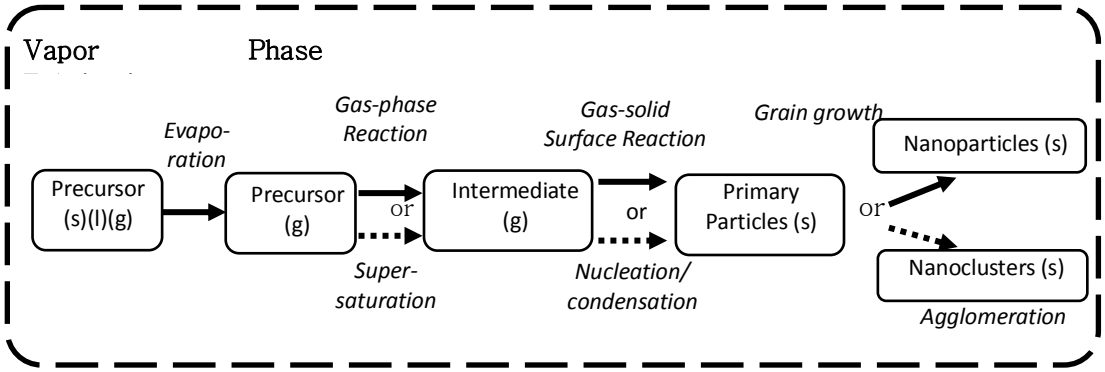

(René Overney/UW Nanothermodynamics and Nanoparticle Synthesis NME 498A/A 2010)

Figure 2: Vapour phase fabrication, reaction process in FSP

The process flow diagram describes the vapor phase which includes:

a. *Initial stage – precursor vaporization.* The precursor of saturated solution of $AlCl_3$ dissolved in distilled water. The precursor is atomized with an ultrasonic atomizer in a gaseous state fed directly into the premixed flame of oxygen/methane. Particles are reduced to atoms before contact with flame.
b. *Intermediate stage – Gas solid surface*. This is the nucleation process, i.e. process by which the gas clouds or vapor is formed into solids. This phase is continuous resulting in the formation of the finest grains. This generally results in homogenization of grain sizes.
c. *Final stage – Growth Stage.* This is the growth stage. The particles are formed and collected at this stage.

Vapour Phase Growth
The growth rate of vapor condensation:

$$R = \xi A_{NP} \frac{\Delta p}{\sqrt{2\pi m k_B T}}; \quad (1)$$

Flux from kinetic theory is $\Delta p = p_v - p_e$ (1a)

Spherical NP: $A_{NP} = 4\pi d_{NP}$ (1b)

Where:

ξ= condensation coefficient (between 0 and 1)
A_{NP} = surface area of condensate (nanoparticle NP)
m = mass of gas molecule
k_B=Boltmann constant
T = absolute temperature
Δp = Driving force: pressure difference
p_v = instantaneous vapor pressure
p_e = local equilibrium pressure at the growing cluster

DISCUSSION
The resultant flame-sprayed and calcinednano-particles would be characterized by chemical analysis using, X-ray diffraction (XRD), further analysis was done using the XRD measurements.

Calculation of the Crystalline Diameter
Calculation on the diameter of particles was based on Scherrer's equation:

$$D_{hkl} = \frac{0.9\lambda}{\beta_{hkl} Cos\theta} \quad (2)$$

Where:
D_{hkl}= size of the particles
λ = wavelength of the X-ray
β_{hkl}= width of the base of diffraction line at half its maximum intensity.

In Equation (1), it is assumed that the particles were perfectly spherical. The two highest peaks (90) and (100) in the XRD patterns were chosen to calculate the size of the nano-particles.

Measurements of Specific Surface Area
The specific surface area of the powder is estimated from the BET-isotherm, measured by multi-point nitrogen adsorption (Gemini 2630, Micromeretics) at 77K.

If the particles are assumed to be spherical with a known density, a BET-equivalent particle size can be calculated as:

$$d_{BET} = \frac{6}{\rho_p S_A} \quad (3)$$

Where:

ρ_p= solid phase density,
S_A = specific surface area
d_{BET} = equivalent particle size.

The Collision/Coalescence Mechanism of Primary Particle Formation
Industrial flame reactors are operated at high particle concentrations, resulting in high rates of particle collision. Particle size is determined by the rates of particle collision and subsequent coalescence mechanism for particle formation is based on a series of steps assumed to proceed as follows:

a. A chemical (or physical) process converts the aerosol precursor to condensable molecules.
b. The condensable molecules self-nucleates to form a cloud of stable nuclei, which may be single molecules (corresponding to a nucleation process with zero activation energy).
c. Stable nuclei collide and initially, coalesce to form larger particles. The particles may be liquid or solid during the coalescence period.
d. Coalescence ceases or slows significantly, leading to the formation of agglomerated structures.
e. Coalescence and neck formation may continue for particles with the agglomerate structures.

These processes may go on simultaneously. For example, chemical or physical processes may continue to generate condensable monomer molecules throughout the process of particle formation. In this case, after an initial surge of particle formation, further releases of monomer molecules will deposit on existing particles without generating new ones.

The stoichiometry of the reaction (but not the true chemical reaction steps) and be loosely represented by the chemical equations below:

$2H_2O + O_2 \rightarrow H_2O$ (4)

$2AlCl_3 + 3H_2O \rightarrow Al_2O_3 + 3H_{(2)}Cl_{2(g)}$ (5)

RESULTS

The X-Ray Diffraction (XRD) analysis is conducted to determine the phase composition and grain size of the flame spray synthesized nano-particles. The XRD patterns for the investigated samples synthesized at different flame temperature with constant flow rate are shown in Figures 3, 4, and 5.

XRD was also used to investigate changes of phase structures and crystalline sizes of the calcinated agglomerate-free Al_2O_3 nanoparticles. Figure 4.4 shows the plot of identified phase structures. Table 4.1 shows the XRD peak positions and relative intensities of the powder. Figure 4.5, 4.6 and 4.7 shows the variation of relative intensities against peak positions of samples 1, 2, and 3 at temperatures of 450°C, 600°C and 750°C respectively.

The XRD patterns for the investigated sample 1 prepared at 450°C temperature of flame at constant flow rate is shown in Figure 3.

The XRD pattern for the investigated sample 2 prepared at flame temperature of 600°C at a steady flow rate is shown in Figure 4.

Also, XRD pattern for the investigated sample 3 prepared at flame temperature of 750°C at a steady flow rate is shown in Figure 5.

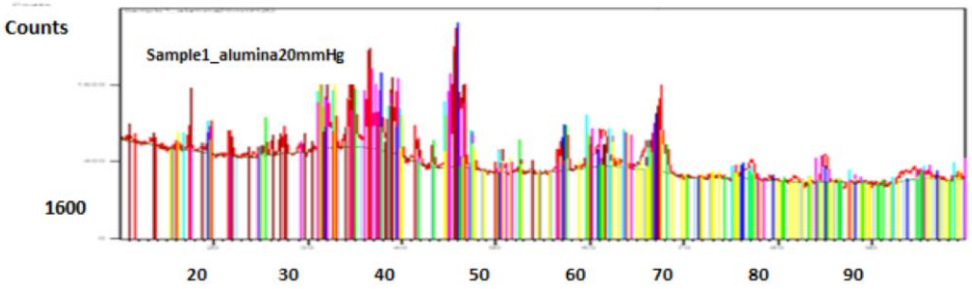

Figure 3: XRD patterns of Al_2O_3nano-sized particles synthesized at flame temperature of 450°C at a constant flow rate. Standard peak position (JCPDS 21-1272) of the Al_2O_3 anatase phase is given in vertical lines.

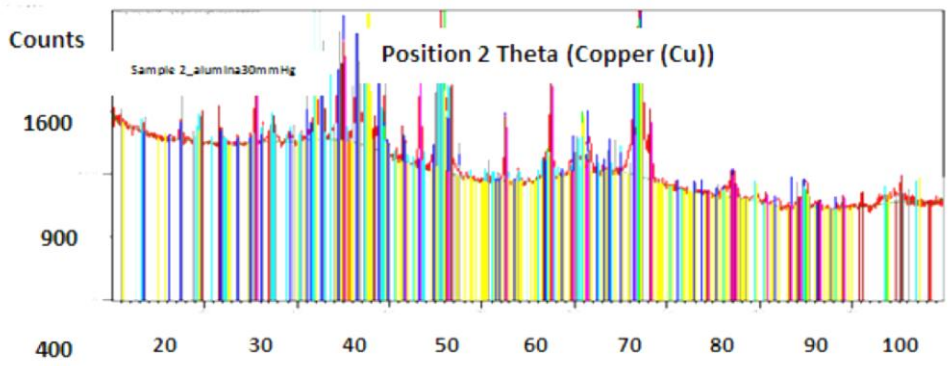

Figure 4: XRD pattern of Al_2O_3nano-sized particles synthesized at flame temperature of 600°C at a steady flow rate. Standard peak position (JCPDS 21-1272) of the Al_2O_3nano-sized particle is given in vertical line

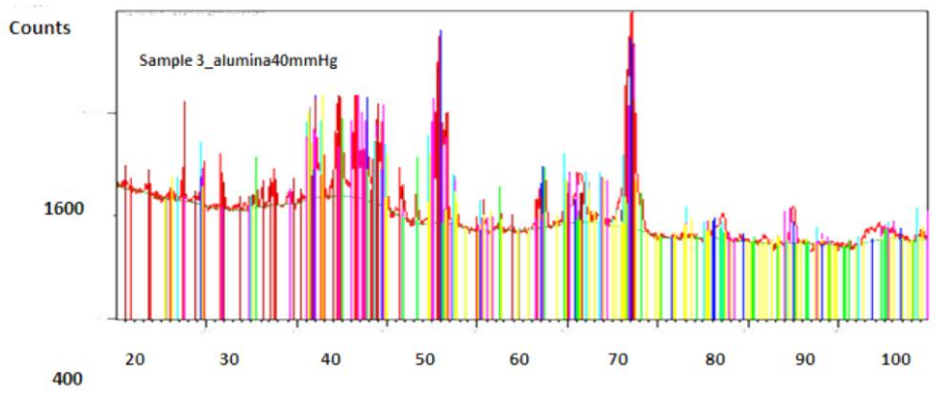

Figure 5: XRD pattern of Al_2O_3nano-sized particles synthesized at flame temperature of 750^{o}C at a steady flow rate. Standard peak position (JCPDS 21-1272) of the Al_2O_3nano-sized particles is given in vertical lines

All diffraction peaks are indexed with the standard JCPDS (21-1272) and found to be corresponding to the pure Anatase and Rutile phases Al_2O_3 crystalline phase.

Determination of the Crystalline Diameter Size

Calculation on the diameter of particles was based on Scherrer's equation (Tok*et al*, 2006):

$$D_{hkl} = \frac{0.9\lambda}{\beta_{hkl} Cos\theta} \qquad \text{(3 above)}$$

Where: D_{hkl}= size of the particles

λ = wavelength of the X-ray

β_{hkl}= width of the base of diffraction line at half its maximum intensity.

Using values of Table 1, row 1, we can obtain the size of particles in nanometers. Using equation 5 above:

The equation proves the assumption that the particles were perfectly spherical. The highest peaks for each synthesized samples (i.e. samples 1, 2, and 3) was chosen to determine the size of the nano-particle. Hence, crystalline minimum diameter size for each sample (i.e. samples 1, 2, and 3) respectively has been found to be about 11.96 nm, 10.39 nm and 11.41 nm, with specimen length respectively.

Table 1: Evaluated mean crystalline size for Samples 1 prepared at flame temperature of 450^{o}C

Sample	Calculated Diameter [nm]	Crystalline	Evaluated Mean Value [nm]	Crystalline
Sample 1	24.2601 14.9615 12.9594 7.9601 14.7465 14.2101 8.2376 13.4583 7.9221 12.9744 9.5118 6.4689 13.4842 10.5002 7.5218 6.9959 10.9242 18.2239		11.96228	

Table 2: Evaluated mean crystalline size for Samples 2 prepared at flame temperature of 600^{o}C

Sample	Calculated Diameter [nm]	Crystalline	Evaluated Mean Value [nm]	Crystalline
Sample 2	7.0364 9.9727 13.1918 11.2590 7.1749 14.2132 10.4482 10.2894 10.1512 13.4571 6.5992 13.0624 6.4664 9.6845 9.7735 8.1532 7.1931 12.0377 9.8004 12.6190 9.4041 16.6343		10.3919	

Table 3: Evaluated mean crystalline size for Samples 3 prepared at flame temperature of 750^{o}C

Samples	Calculated diameter [nm]	crystalline	Evaluated Mean Value [nm]	Crystalline
Sample 3	13.1893 17.5918 16.8113 11.2474 8.6149 8.3540 10.1501 13.3939 13.0626 6.4659 9.6692 9.7786 10.1759 5.4061 16.0257 12.6623 9.4184		11.41242	

X-Ray Diffraction Graph Analysis

The XRD measurements were performed on a thin powder layer deposited on steel sheet. The simulation graph for each samples according to their flame temperature deposition (i.e. 450 ^{o}C, 600 ^{o}C and 750 ^{o}C) are shown in figure 6, 7 and 8 respectively, where only the major peaks of the resulting spectrum are considered. As it may be seen, the anatase phases (66.3%, 89% and 99%) are largely prevalent in the collected powder and rutile phases (10%, 9% and 3%) at flame temperatures of 450 ^{o}C, 600 ^{o}C and 750 ^{o}C respectively. It is worthwhile to note that anatase is generally considered as the most active phase.

SAMPLE 1 (450^{O}C flame temperature)

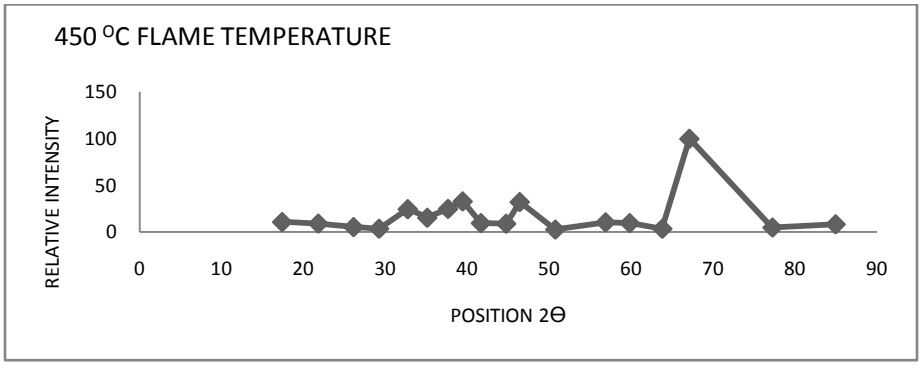

Figure 6: Simulation graph of the XRD spectrum of the synthesized nano alumina at 450^{o}C flame temperature showing both anatase and rutile relative intensities of powder particles (A=Anatase and R=Rutile)

Table 4: Pattern values for Sample 1 (450^{o}C flame temperature)

VISIBLE REFERENCE CODE	SCORE	COMPOUND NAME	DISPLACEMENT [^{O}2TH]	SCALE FACTOR	CHEMICAL FORMULA
00-016-0394	57	**α**-Al_2O_3	0.000	0.830	Al_2O_3
00-053-1247	55	Strontium Chromium	0.000	0.595	$Sr_2Cr\ NbO_{5.53}$
00-046-1215	67	**α***- Al_2O_3	0.000	0.710	Al_2O_3
00-009-0440	25	β- Al_2O_3	0.000	0.328	Al_2O_3
00-046-1131	44	**α**- Al_2O_3	0.000	0.703	Al_2O_3
01-086-1410	36	β- Al_2O_3	0.000	0.385	Al_2O_3
00-021-0010	37	**α**-Al_2O_3	0.000	0.652	Al_2O_3
01-073-6579	43	γ- $Al_{2.66}O_4$	0.000	0.784	$Al_{2.66}O_4$
01-088-0826	41	γ- $Al_{2.66}O_4$	0.000	0.197	Al_2O_3

SAMPLE 2 (600 ^{O}C flame temperature)

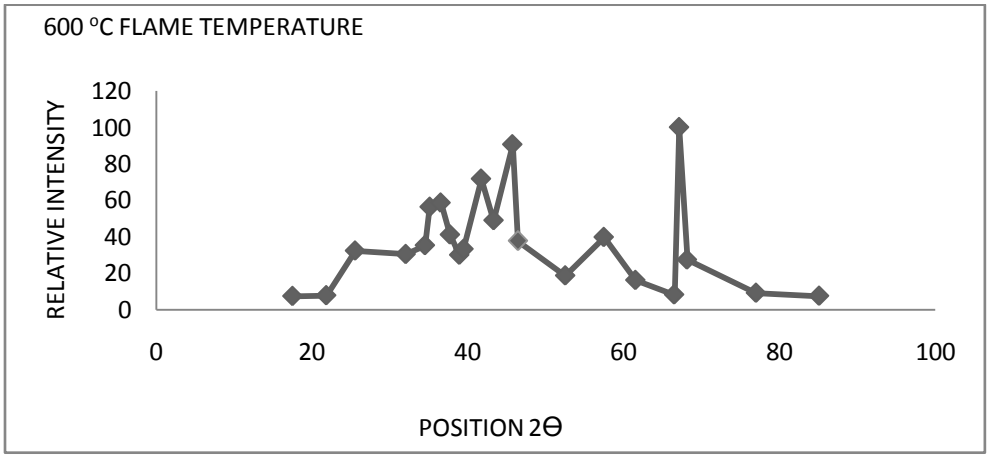

Figure 7: Simulation graph of the XRD spectrum of the synthesized nano alumina at 600 ^{o}C flame temperature showing both Anatase and Rutile Relative intensities of powder particles (A=Anatase and R=Rutile)

Table 5: Pattern values for Sample 2 (at 600 ^{o}C flame temperature)

VISIBLE REFERENCE CODE	SCORE	COMPOUND NAME	DISPLACEMENT [^{O}2TH]	SCALE FACTOR	CHEMICAL FORMULA
00-016-0394	57	**α**-Al_2O_3	0.000	0.830	Al_2O_3
01-077-2188	41	Corundum chromian	0.000	0.268	$Al_{1.54}O_3Cr._{46}$
01-086-1410	36	β- Al_2O_3	0.000	0.385	Al_2O_3
00-021-0010	37	**α**-Al_2O_3	0.000	0.652	Al_2O_3
01-073-6579	43	γ- $Al_{2.66}O_4$	0.000	0.784	$Al_{2.66}O_4$
01-088-0826	41	γ- $Al_{2.66}O_4$	0.000	0.197	Al_2O_3
01-081-1667	56	**α**- Al_2O_3	0.000	0.490	Al_2O_3
01-079-1558	45	ã-$Al_{2.144}O_{3.2}$	0.000	0.630	$Al_{2.144}O_{3.2}$
01-071-1124	47	corundum HP, ruby HP	0.000	0.399	Al_2O_3
01-070-9085	42	alumina, syn	0.000	0.701	$(Al_2O_3)_{1.333}$

SAMPLE 3 (750 ^{O}C flame temperature)

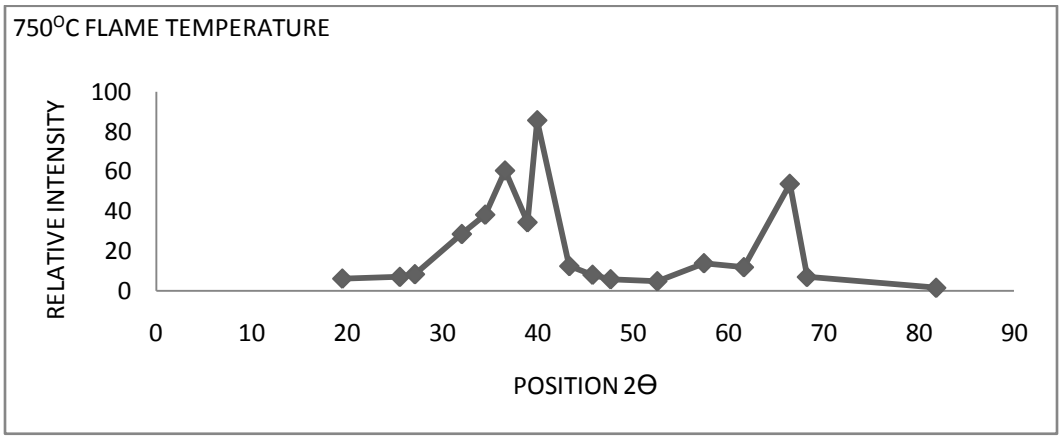

Figure 8: Simulation graph of the XRD spectrum of the synthesized nano alumina at 750^{o}C flame temperature showing both Anatase and Rutile Relative intensities of powder particles (A=Anatase and R=Rutile)

Table 6: Pattern values for Sample 3 (750 ^{o}C flame temperature)

VISIBLE REFERENCE CODE	SCORE	COMPOUND NAME	DISPLACEMENT [^{O}2TH]	SCALE FACTOR	CHEMICAL FORMULA
00-020-0660	63	**α**-Mg $Al_{26}O_{40}$	0.000	00.857	Mg $Al_{26}O_{40}$
01-077-2188	59	Corundum chromian	0.000	0.668	$Al_{1.54}O_3Cr._{46}$
00-036-0050	45	Aluminum Oxide Nit.	0.000	0.659	Al_3O_3N
00-046-1131	37	**α**- Al_2O_3	0.000	0.698	Al_2O_3
00-021-0010	38	**α**- Al_2O_3	0.000	0.663	Al_2O_3
01-080-0786	58	**α**- Al_2O_3	0.000	0.506	Al_2O_3
00-042-1468	55	alumina, alundum,	0.000	0.506	Al_2O_3
00-056-1186	48	**α**- Al_2O_3	0.000	0.804	Al_2O_3
01-074-2206	47	Aluminum Oxide	0.000	0.816	$(Al_2O_3)_{0.5333}$
00-046-1215	60	**α**- Al_2O_3	0.000	0.696	Al_2O_3

CONCLUSION

This work focused and has successfully shown that Al_2O_3 nanoparticles can be successfully synthesized with the FPS method, it can be seen that this method has the flexibility of easily synthesizing other nanoparticles by flame spraying other metal chlorides that have a low boiling point. It is novel and easy way of synthesizing nanoalumina, therefore, cost effective for the mass production of nanoalumina in industries. XRD readings were also used to obtain the phase shift in diffraction of

the nanoparticles and data obtained was calculated to get the average crystalline diameter value, the mean crystalline diameter of the nanoparticles were obtained to be for Sample 1, 2 and 3 to be 11.96nm, 10.39nm and 11.41nm respectively.Further tests will be devoted to the improvement of the apparatus setup and to the synthesis of other types of nanoparticles.

REFERENCES

Madler, L., Kammler, H.K., Mudler R., and Pratsinis S. G., Journal of Aerosol Science 2002, 369.

Madler, L., Stark, W.J. and Pratsinis, S.E., Mater, J., Research 18, 2003, 115.

Messing, G.L., Zhang, S.C., Jayanthi, G.V., (1993). Ceramic powder synthesis by spray pyrolysis, Journal of American Ceramic Society 76: 2707–2726.

Overney, R. (2010).Nanothermodynamics and Nanoparticle Synthesis.University of Washington, University Press.

Pathak, L.C., Singh, T.B., Das, S., Verma, A.K., Ramachandrarao, P., (2002). Effect of pH on the combustion synthesis of nano-crystalline alumina powder, Material Lettering. 57 380–385.

Pratsinis S.E. (1998). Flame aerosol synthesis of ceramic powders, programme energy combustion science, 24:197-219, 1998.

Stark, W.J. and Pratsinis, S.E., Powder Technology. 126, 2002, 103.

Stark, W.J., Wegner, K., Pratsinis, S.E. and Baiker, A. 2001, 182.

Stark, W.J., Kammler, H.K., Strobel R., Gunther, D., Baiker, A and Pratsinis, S.E. Industrial Engineering chemistry Research, 2002, 41.

Strobel, R., Krumeich,F., Stark W.J., Pratsinis, S.E. and Baiker, A. Journal catal. 222, 2004, 307.

Strobel, R., Grunwaldt, J.D., Gamenzind, A. and Baiker, A., Pratsinis, S.E. Chemical Engineering Science, 2003; 1969.

Strobel, R. &Pratsinis, S.E. (2009). Flame Synthesis of Platinum Group Metals for Catalysis and Sensors. Novel Flame Processes allow Synthesis of supported PGMs in a Single Step. Platinum Metals Revised. 53(1), 11-20.
DOI:10.1595/147106709X392993

Strobel, R. Pratsinis, S.E. and Baiker, A. Journal Material Chemistry 15; 2005: 605.

Strobel, R., Krumeich, F., Stark, W. J., Pratsinis and Baiker, A., 2003, 115.

Tikkanen, J. (1999) Liquid flame spray development and its applications.Ph.D. Thesis Tampere University of Technology.

Tok, A.I.Y., Boey, F.Y.C., Zhao, X.L., (2006).Novel Synthesis of Al2O3 Nano-Particles by Flame Spray Pyrolysis. School of Materials Science & Engineering, Nanyang Technological University, Nanyang Avenue, Singapore 639798, Singapore. http://www.mse.ntu.edu.sg/aboutus/organisation/documents/files/staff/publications/j16.pdf

Wu, Y.Q., Zhang, Y., Huang, X., Guo, J., (2001). Preparation of plate like nano alpha alumina particles.Ceramic International. 27:265-268.

Wu, M.K., Windler R.S., Steiner, C.K.R., Bor, T., and Friedlander, S.K. 1993.Controlled synthesis of nanosized particles by aerosol processes. Aerosol Science Technology 19:527.

Yang, P. and Luzzi, D.E. "Nanotechnology."Microsoft® Encarta® 2009 [DVD]. Redmond, WA: Microsoft Corporation, 2008. Microsoft ® Encarta ® 2009. © 1993-2008 Microsoft Corporation. All rights reserved.

Zuo, Y., Zhao, Y., Li, X., Li, N., Bai, X., Qiu, S., Yu, W., (2006).Synthesis of alumina nanowires and nanorods by anodic oxidation method, Material Lettering, 60(24), 2937.